

# Suppression of Co-Channel Interference in High Duty Ratio Pulsed Radar Receivers

*C M Alabaster\**

*\*White Horse Radar Limited, UK, email: clive@whradar.com*

**Keywords:** Co-Channel Interference, Pulsed Radar, Receiver, High duty ratio.

## Abstract

This paper describes a technique for the suppression of interference, particularly co-channel components arising from interference on neighbouring channels, within a pulsed radar receiver operating on a high duty ratio. The technique employs two RF switches with a band pass filter between them and nesting the gating control of the second switch to lie within the gating control of the first switch. Simulations indicate that rejection of in-band interference components arising from interference that is offset by 60MHz from the channel centre frequency some 20dB greater than that of a conventional filtering is possible. The technique is most effective at high duty ratios.

## 1 Introduction

One of the most damaging forms of interference for any radar is co-channel interference from another, similar radar, since the interference signal closely resembles that expected by the victim radar. Interference on a neighbouring channel frequency but within the front-end bandwidth of the radar can be accepted into the radar causing saturation of front-end components and intermodulation products within the channel bandwidth. Furthermore, the receiver protection switching can modulate the interference resulting in additional frequency components within the channel bandwidth. Consequently, the interference can cause a flood of false alarms, saturate the processing and corrupt the operation of the constant false alarm rate (CFAR) detector. To combat this problem, a radar may cancel interference signals within its signal processor or use auxiliary antenna cancellation techniques, or steerable antenna nulls, in the direction of the interference sources; orthogonal waveforms may be used by like radars operating within range of each other in order to suppress mutual interference. It would, however, be preferable to reject interference within the receiver *before* it reaches the processor since this reduces the processing burden, does not distort antenna beams if steered close to nulls in their radiation patterns and does not require coordination of waveforms between similar radars.

A simple technique is described here that can provide high levels of interference rejection in pulsed radars operating on a high duty ratio. High duty ratios are often associated with

high PRF waveforms but this need not always be the case. The solution uses standard components within the radio frequency (RF) radar receiver; namely two RF switches and a band pass filter (BPF) between the two switches. The first switch pulse modulates the interference at the pulse repetition frequency (PRF) of the victim radar and the BPF passes only high order PRF components that are manifest as impulses of in-band interference at the switching edges of the first switch. The gating control of the second switch is nested within the gating control of the first switch such that the impulses of interference are gated out. The critical and novel elements described here are the relative timings of the switch gating signals and the filter requirements.

Section 2 describes the technique in more detail and section 3 provides an analytical basis. The fourth section describes details of a simulation, including some simulation results. Finally, section 5 draws some conclusions.

## 2 Description of the Technique

### 2.1 The Problem

Consider a situation whereby a pulsed radar is receiving interference from another pulsed radar. The situation is portrayed in Figure 1 for a source of pulsed interference and a victim receiver both operating on nominally the same PRF with a 50% duty ratio. The top trace (a) in Figure 1 shows the transmitted pulses from an interference source. The middle trace (b) of Figure 1 is the gating function of a victim receiver that, when low, isolates the receiver during the transmission of its own pulses and, when high, permits the reception of signals. The bottom trace (c) of Figure 1 shows the non-eclipsed fragments of the interference pulses that are accepted into the victim receiver. Since the timings of the transmitted pulses and the gating of the victim receiver will, in general, be asynchronous, in addition to an unknown range delay between the two, there will be a random timing offset between the two. This means that only fragments of the transmitted pulses will be received corresponding to periods when the transmitted pulses are present during the receiving time of the victim radar. For 50% duty ratios, one edge of the fragment of interference will be defined by the transmitted modulation (the trailing edge, as shown in Figure 1) and the other edge will be defined by the receiver gating (the leading edge, as shown in Figure 1). Although the two radars may both be running on notionally the same PRF, in practice, there

will always be a slight difference in their PRFs. Furthermore, the range between the transmitter of the interference and the receiver may constantly be changing. Both the PRF difference and changing range will ensure that the timings of the transmitted pulses and receiver gating drift in and out of phase with each other and, as a result, the width of the fragment of interference is constantly changing. Additionally, the definition of the leading/trailing edges of this fragment swaps periodically between the transmitted modulation and receiver gating. The bandwidth of the interference is given by the reciprocal of the pulse fragment width and will therefore constantly be changing. The rate at which the spectrum of the interference decays at higher offset frequencies from its carrier frequency depends on the rise and fall times of the transmitted modulation and receiver gating. Since both these signals tend to have sharp edges, there will be considerable spectral spread into neighbouring channels. As the duty ratio of the transmitter and receiver reduce, or the width of the transmitted pulses becomes much less than the victim receiver's open time, both edges of the interference pulses become more likely to be defined by the transmitted modulation. Notwithstanding this, there is always some likelihood that fragments of interference will have one edge defined by the receiver gating. A complete solution to mutual interference must therefore address both the transmission of pulses and the receiver.

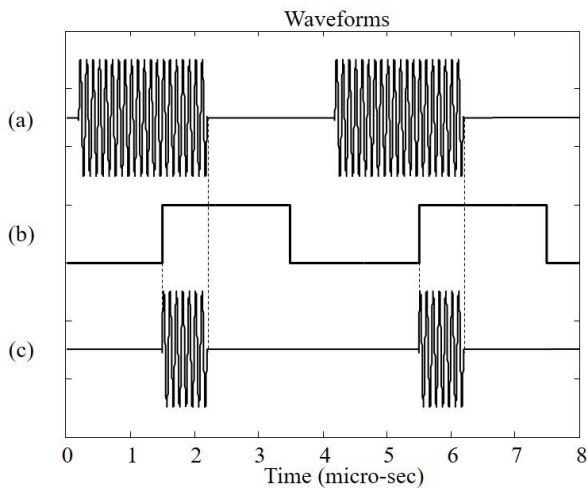


Figure 1: Interference from pulsed radar operating on a 50% duty ratio. (a) Pulsed interference, (b) Gating control of victim receiver (*high* = receiver open, *low* = receiver closed), (c) Fragment of interference pulse accepted into receiver.

## 2.2 The Solution

The classic solution to limit the spectral spread of transmitted pulses is to shape the pulses with a weighting function [1]. This extends the rise and fall times of the transmitted pulses. Even the simple expedient of imparting a cosine function rise and fall (voltage) profile over the first and last 20ns of a 2.5µs pulse can reduce the spectral envelope by 15dB at an offset frequency of 60MHz compared with 2ns rise and fall times.

If, however, only one edge of the pulse has the 20ns cosine profile and the other edge has a 2ns rise time, then the improvement is only 4.5dB at a 60MHz offset frequency. Clearly, it is important that both edges of the interference pulse fragment be shaped in order to reduce co-channel interference.

Whilst it is possible to shape the receiver gating function in much the same way that transmitted pulses may be shaped, it is not always practical to do so. Firstly, if the interference is powerful enough to drive any subsequent amplifier stages into saturation, the profiled edges will be 're-sharpened'. Secondly, the extended rise and fall times on the receiver gating function increase eclipsing losses and the minimum range [2].

The reduction in spectral spread can be imparted within the receiver using a combination of two switches with a filter between them. A block diagram of a typical superheterodyne receiver front-end is shown in Figure 2. The crucial and novel elements are the two switches, and specifically, the timing controls to these switches, with the band pass filter (BPF) sandwiched between them and these components are highlighted using the light grey shading in Figure 2. Any pulsed radar receiver requires a protection switch before the low noise amplifier (LNA) in order to isolate it from damaging levels of transmitter leakage power during its transmitted pulses; this forms the first RF switch. Received signals are then amplified in the LNA and down-converted to an intermediate frequency (IF) using a mixer. The BPF is designed to filter out interference falling outside the channel bandwidth of the radar and so may typically have a bandwidth of a several MHz; it is not intended to be the matched filter, which would typically come further along the processing chain. The BPF is more easily implemented in the IF signal path, rather than at the incoming (microwave) RF section, since it requires a more modest *Q*-factor here. The isolation provided by the protection switch may typically be around 60dB and, although adequate to protect the LNA from saturation, still results in a detectable level of transmitter leakage power within the receiver. This should be removed using an additional high isolation switch before the high gain amplifier chain; this is the second switch shown on the right of Figure 2.

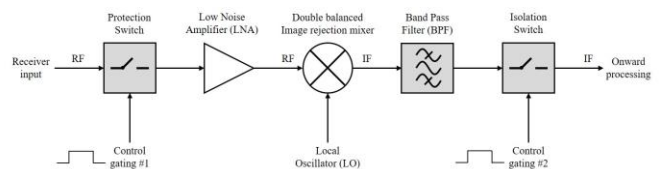


Figure 2: Radar superheterodyne receiver front-end block diagram.

In order to isolate the receiver effects from those of shaping the transmitted pulses, it is most convenient to consider continuous wave (CW) interference. If CW interference is received on a neighbouring channel it should be subject to a

high degree of rejection by the BPF, however, the action of the protection switch pulse modulates the interference at the receiving system's PRF and causes significant spectral spread into the pass band of the BPF, especially if the protection switch imparts fast rise and fall times. Ironically, the protection switch has exacerbated the problem. The BPF passes high order PRF harmonics that result in an output signal comprising short bursts (*impulses*) of interference occurring at the rising and falling edges of the pulses of interference, i.e. at the rising and falling edges of the gating function of the protection switch. The BPF has *differentiated* the pulses of interference. The duration of these 'impulses' is proportional to the rise and fall times of the protection switch and inversely proportional to the bandwidth of the BPF and the frequency of the interference; they may typically last for a few tens of nano-seconds for a filter bandwidth of 25-30MHz. The high isolation switch that follows the BPF must now have a gating control nested within that of the protection switch such that these impulses are gated out. The gating timings are illustrated in Figure 3 and a close-up view of the rising and falling edges with 30ns nested timings is shown in Figure 4. In gating out the impulses, the in-band interference is removed. Should this interference not be removed it could cause false target indications, mask smaller genuine target responses falling coincident in range and velocity as the interference, sap effort from the tracker which may attempt to track these responses and corrupt the operation of the constant false alarm rate (CFAR) detection; in short, the interference could have similar effects as would false target jamming. The only in-band interference that remains are high order PRF harmonics associated with the filtered interference. Consequently, the in-band interference is reduced by approximately the level of the filter rejection at the centre frequency of the interference and will be significantly lower than that seen on the BPF output, or if the gating function to the high isolation switch was not properly nested within the gating function of the protection switch. The exact timings in a practical system would have to be adjusted to account for the group delay between the two switches. The (small) penalty paid for the high degree of interference rejection is the slightly increased dead time due to the nesting and subsequent increases in eclipsing losses. It is therefore advantageous to ensure that these impulses be as short-lived as possible, such that the dead time due to switch nesting may be minimised, and so this demands rapid switching of the protection switch, a wide pass band of the BPF and minimal dispersion in all the circuits between the two switches. To this end, the BPF should have a linear phase filter response across its (wide) pass band, which is most readily achieved if its pass band is centred at a high frequency, i.e. a high value of IF is used (VHF (30-300MHz) or UHF (300-1000MHz) being better than HF (3-30MHz) [3]).

The design of the BPF is crucial to the success of the interference rejection. The impulses represent the filter's transient response to the rising and falling edges of the pulse of out-of-band interference. The duration of the impulses is reduced for a large offset between the filter pass band and the interference and for a wide pass band. The pass band should

not be so wide, however, that it compromises the rejection of out-of-band interference. Resistive filter losses introduce damping which lengthens the impulses; dispersion in the filter, and other components before the isolation switch, also stretches the impulses and should be avoided.

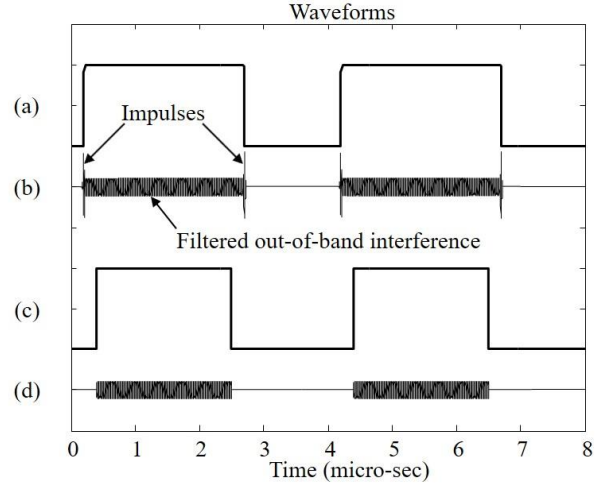


Figure 3: Signal waveforms. (a) protection switch gating, (b) BPF output signal, (c) isolation switch gating, (d) signal at isolation switch output.

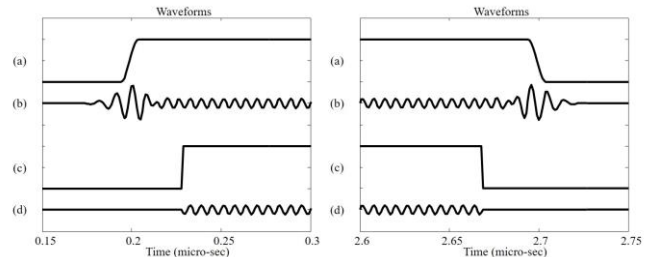


Figure 4: Close-up of waveforms at switching rise/fall times. (a) protection switch gating, (b) BPF output signal, (c) isolation switch gating, (d) signal at isolation switch output.

### 3 Theory

The processing of a received signal by the analogue receiver components highlighted in grey in Figure 2 entails switching between the time and frequency domains. The gating function provided by the two switches is most conveniently applied in the time domain whereas the filtering function of the BPF is most conveniently applied in the frequency domain. The Fourier transform, together with the inverse Fourier transform, enables one to transform from the time ( $t$ ) to frequency ( $\omega$ ) domains and back again [4].

Let the CW interference signal be given by:

$$s_0(t) = \cos(\omega_i t) \quad (1)$$

where  $\omega_i$  is the angular frequency of the interference.

It is necessary to consider just a single cycle of the pulsing operation of the protection switch which can therefore be represented by the idealised time gating function:

$$g_1(t) = \begin{cases} 1 & 0 \leq t \leq \tau \\ 0 & \text{elsewhere} \end{cases} \quad (2)$$

This switch modulates the interference signal with zero insertion loss when the switch is closed and infinite isolation when open. It results in a rectangular pulse of interference having a pulse width,  $\tau$ , of infinitely fast rise and fall times. The pulse modulated interference signal on the switch output is therefore:

$$s_1(t) = s_0(t) \cdot g_1(t) = \begin{cases} \cos(\omega_i t) & 0 \leq t \leq \tau \\ 0 & \text{elsewhere} \end{cases} \quad (3)$$

(The amplification and down-conversion process is inconsequential to the rejection of interference and so the same interference carrier frequency has been retained throughout.) The  $s_1(t)$  signal is a single pulse of the original interference from time,  $t = 0$  to  $t = \tau$ .

The spectrum of this signal is given by its Fourier transform, which is defined as:

$$S_1(\omega) = \mathcal{F}\{s_1(t)\} = \int_{-\infty}^{+\infty} s_1(t) e^{-j\omega t} dt \quad (4)$$

In this case, the function  $s_1(t)$  is given by the product of two functions, so:

$$S_1(\omega) = \mathcal{F}\{s_0(t) \cdot g_1(t)\} = S_0(\omega) * G_1(\omega) \quad (5)$$

where  $S_0(\omega)$  represents the Fourier transform of  $s_0(t)$ ,  $G_1(\omega)$  represents the Fourier transform of  $g_1(t)$  and  $*$  represents the convolution of the two. In practice, it is not necessary to use convolution since the Fourier transform of  $s_1(t)$  may be derived directly from the definition of the Fourier transform given by Equation (4) over three time intervals;  $t < 0$ ,  $0 \leq t \leq \tau$  and  $t > \tau$ . The resulting spectrum is given by:

$$S_1(\omega) = \frac{-j\omega + j\omega_i e^{j\omega_i \tau} \cos(\omega_i \tau) + \omega_i e^{j\omega_i \tau} \sin(\omega_i \tau)}{\omega_i^2 - \omega^2} \quad (6)$$

This is the classic sinc function spectrum centred at  $\omega_i$  with an angular frequency offset to the nulls at multiples of  $2\pi/\tau$ .

Should the analysis be extended to capture at least two periods of the gating function,  $g_1(t)$ , its periodicity would be evident and would result in a set of discrete spectral responses offset by harmonics of the PRF and whose envelope conforms to the sinc function given by Equation (6).

Let the BPF have an idealised transfer function given by:

$$F(\omega) = \begin{cases} \cos \beta + j \sin \beta = e^{j\beta} & \omega_L \leq \omega \leq \omega_U \\ 0 & \text{elsewhere} \end{cases} \quad (7)$$

where  $\omega_L$  and  $\omega_U$  are the lower and upper frequency limits of the pass band, respectively, and  $\beta$  is the phase constant of the filter. Within its pass band, the filter has a magnitude response of 1 and a phase response of  $\beta$ . Thus, the filter has a rectangular response of zero pass band insertion loss and infinite stop band isolation and has a linear phase response within its pass band; the filter is therefore non-dispersive. It may be assumed that  $\omega_i$  is well outside the pass band,  $\omega_L$  to

$\omega_U$ , and so the filter passes only low-level, high order sidelobes of the sinc function that are offset well away from  $\omega_i$  represented by Equation (6).

The filter output therefore has a spectrum given by:

$$S_2(\omega) = S_1(\omega) \cdot F(\omega) \quad (8)$$

Substitution of Equations (6) and (7) into Equation (8) gives:

$$S_2(\omega) = \frac{-j\omega e^{j\beta}}{\omega_i^2 - \omega^2} \left[ 1 - e^{j\omega \tau} \cos(\omega_i \tau) + \frac{j\omega_i}{\omega} e^{j\omega \tau} \sin(\omega_i \tau) \right] \quad (9)$$

$$S_2(\omega) = 0 \quad \text{elsewhere}$$

The time domain representation of this signal may be obtained via an inverse Fourier transform, i.e.:

$$s_2(t) = \mathcal{F}^{-1}\{S_2(\omega)\} = \frac{1}{2\pi} \int_{-\infty}^{+\infty} S_2(\omega) e^{j\omega t} d\omega \quad (10)$$

In this case, the upper expression for  $S_2(\omega)$  given by Equation (9) can be substituted in Equation (10) and the limits of integration can be reduced to  $\omega_L$  and  $\omega_U$ . Note also that:

$$\beta = \frac{\omega}{v_p} \quad (11)$$

where  $v_p$  is the phase velocity through the filter. The time domain representation of the filter output is therefore given by:

$$s_2(t) = \frac{1}{2\pi} \int_{\omega_L}^{\omega_U} \left[ -j\omega e^{j\omega(t+1/v_p)} + j\omega_i e^{j\omega(t+\tau+1/v_p)} \cos(\omega_i \tau) + \dots \right. \\ \left. \dots \omega_i e^{j\omega(t+\tau+1/v_p)} \sin(\omega_i \tau) \right] / (\omega_i^2 - \omega^2) d\omega \quad (12)$$

This signal is incident on the isolation switch. Again, it is necessary to consider just a single cycle of the pulsing operation of the isolation switch which can therefore be represented by the idealised gating function:

$$g_2(t) = \begin{cases} 1 & t_n \leq t \leq \tau - t_n \\ 0 & \text{elsewhere} \end{cases} \quad (13)$$

where  $t_n$  is the nesting margin of the isolation switch within the timings of the protection switch,  $g_1(t)$ . The gating function to the isolation switch is a pulse of width  $\tau - 2t_n$  delayed by  $t_n$  with respect to  $g_1(t)$ . As for the protection switch, the isolation switch exhibits infinitely fast rise and fall times, zero insertion loss when the switch is closed and infinite isolation when open and it provides further modulation of the interference signal.

The waveform on the output of the isolation switch is therefore given by:

$$s_3(t) = s_2(t) \cdot g_2(t) \quad (14)$$

The spectrum of the output signal is given by the Fourier transform of  $s_3(t)$ , i.e.:

$$S_3(\omega) = \mathcal{F}\{s_3(t)\} = S_2(\omega) * G_2(\omega) \quad (15)$$

where  $G_2(\omega)$  represents the Fourier transform of  $g_2(t)$ .

Ascertaining the spectra and waveforms of the signals on the input and output of the isolation switch entails an evaluation of the integral of Equation (12). The precise nature of these signals depends on the values of  $\omega_i$  and  $\tau$  with respect to  $\omega_L$  and  $\omega_U$ . Of particular interest here, is the case of both  $\omega_L$  and  $\omega_U$  being offset from  $\omega_i$  by many times  $2\pi/\tau$ , i.e. typically,

$$|\omega_i - (\omega_L, \omega_U)| > 100 \times 2\pi/\tau.$$

Evaluation of Equation (9) and the integral of Equation (12) is awkward but some general trends may be observed for the particular choice of parameter values of interest here that aid understanding. Equation (9) is of the general form:

$$\frac{-j\omega + a}{(-j\omega + a)^2 + \omega_c^2} (1 - e^{j\omega\tau}) \quad (16)$$

The  $e^{j\beta}$  term in Equation (9) merely introduces a phase offset to the spectrum or a time shift equivalent to the delay through the filter into the waveform, Equation (10), and may be ignored here. The inverse Fourier transform of Equation (16) represents the waveform of an exponentially decaying cosine wave starting at time  $t = 0$  followed by an exponentially decaying negative cosine wave starting at time  $t = \tau$ . The frequency of the cosine waves is given by  $\omega_c$  and the factor ‘ $a$ ’ is the time constant of the exponential decay and will be large and positive for a wide pass band filter centred well away from the carrier frequency of the interference i.e.:

$$|\omega_U - \omega_L| \text{ is large and } |\omega_i - (\omega_L, \omega_U)| > 100 \times 2\pi/\tau.$$

The exponentially decaying cosine waves are the under-damped transient responses of a resonant circuit, i.e. the response of the ideal, loss-less filter to the rising and falling edges of the input pulse. The frequency,  $\omega_c$ , corresponds to the resonant frequency of the circuit, i.e. the centre frequency of the filter pass band. The duration of a filter’s response is given by the inverse of its bandwidth, therefore  $a \propto |\omega_U - \omega_L|$ . As the filter bandwidth increases, ‘ $a$ ’ becomes increasingly large and the exponential decay becomes more rapid with the result that the waveform tends towards a positive impulse at  $t = 0$  and a negative impulse at  $t = \tau$ . This waveform represents the differential of the input pulse whose spectrum is of the form:  $1 - e^{j\omega\tau}$ . It may therefore be understood that, for the particular choice of parameters described here, the waveform,  $s_2(t)$  approximates the differential of the  $s_1(t)$  pulse and resembles the impulses shown in Figure 4, trace (b).

The exponentially decaying cosine ‘impulses’ reduce to 37% of their initial amplitude after a time  $1/(\omega_U - \omega_L)$ . Setting the nesting offset to the inverse of the BPF bandwidth,  $t_n = 1/(\omega_U - \omega_L)$ , enables waveform  $g_2(t)$  to gate out most of the impulses. Increasing  $t_n$  to  $2/(\omega_U - \omega_L)$  allows the impulses to decay to 14% of their initial amplitude, and so more of the impulses are gated out but the dead time and eclipsing losses are doubled. The waveform on the isolation switch output is now very low:  $s_3(t) \approx 0$  for all  $t$ . In this way, significant rejection of the interference within the pass band can be achieved.

## 4 Simulation Results

The signals within the IF section of a hypothetical receiver have been simulated in accordance with the techniques and theory described in the earlier sections. An 8 pole Butterworth filter design has been modelled. A high PRF with a high duty ratio is assumed and would be typical parameters for a high PRF air-to-air velocity search mode of an airborne intercept or fire control radar [5]. The following parameters have been assumed:

• PRF of receiver	250 kHz
• Duty ratio	37.5%
• (receiver open time)	2.5 $\mu$ s)
• IF centre frequency	100 MHz
• BPF insertion loss at 100MHz	1.6 dB
• BPF 3dB bandwidth	27.5 MHz
• Interference centre frequency in IF (i.e. 60MHz above IF centre)	160 MHz
• BPF insertion loss at 160MHz	26.0 dB
• (Rejection wrt to pass band)	24.4 dB)

It was further assumed that the protection switch had a rise and fall (voltage) profile of a cosine function over 10ns. The isolation switch had a 1ns rise and fall time that was nested 30ns within the 50% points of the rise and fall of the protection switch edges (Figure 4). The fast rise and fall times of the isolation switch was intended to give rise to the slowest spectral decay in the interference and hence the most pessimistic result for interference rejection; slower rise/fall times would result in reduced in-band interference. The extra 30ns nesting margin at the beginning and end of each receiving period incurs a dead time totalling 60ns. This dead time reduces the receiver open time to  $2.5\mu\text{s} - 60\text{ns} = 2.44\mu\text{s}$  that results in an extra eclipsing loss of:  $20 \cdot \log_{10}(2.44/2.50) = 0.21\text{dB}$ . A smaller increase in eclipsing loss would be incurred at a lower PRF.

The spectra of the various signals are shown in Figure 5. These spectra were obtained via a uniformly weighted FFT over two complete cycles of the receiver pulsed waveform (8 $\mu$ s). The interference, pulse modulated by the protection switch, and down-converted by the mixer, is shown in the dark blue and its peak level at 160MHz is normalised to 0dB. Its envelope at 100MHz is at -56.5dB and is due entirely to the pulse modulation imparted by the protection switch. The filter characteristic in deciBels is shown in red. The filter provides 24.4dB rejection of interference at +60MHz offset from its centre frequency. The green spectrum corresponds to the interference signal seen on the output of the BPF. Its peak at 160MHz is at -26.04dB and corresponds to the filter insertion loss at this frequency. Its envelope at 100MHz is at -58.1dB which is only 1.6dB lower than the interference level at the IF centre frequency seen at the mixer output (due to the 1.6dB insertion loss of the BPF at 100MHz). This illustrates that the filter will prevent the out-of-band interference from saturating further amplification and processing stages but provides almost no rejection of in-band interference components incurred by the pulsing of the protection switch. The interference seen on the isolation switch output is shown

in cyan and has a peak level of -26.26dB at 160MHz. The small decrease with respect to the BPF output (green) of 0.22dB is due to the slight reduction in the width of the interference pulse, totalling 60ns, due to the 30ns of nesting at each edge, and is consistent with the extra eclipsing loss. From the lower trace of Figure 4, one may observe how the impulses of in-band interference have been removed, leaving the (suppressed) pulse modulated 160MHz signal. Its envelope at 100MHz is at -79.3dB, which shows a 21.2dB decrease with respect to the interference at 100MHz on the filter output (green). The 21.2dB improvement is somewhat less than the 24.4dB rejection provided by the filter at 60MHz offset; the discrepancy being due to the slower decay of the spectrum due to the faster edges of the isolation switch (plus a minor discrepancy due to the slight change in its pulse width, as noted earlier).

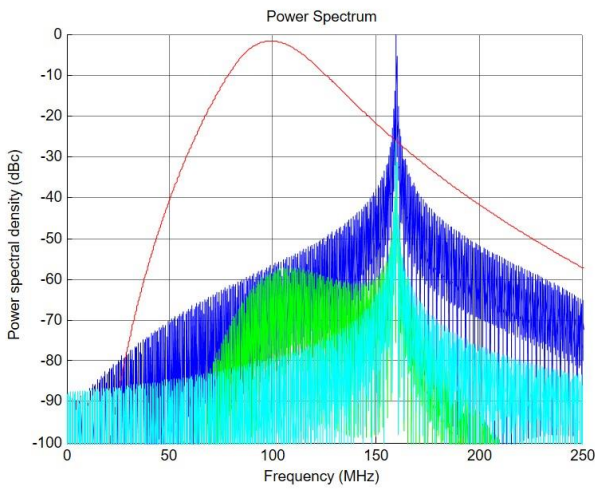


Figure 5: Signal spectra. *Blue* = interference at mixer output, *Red* = filter characteristic, *Green* = interference at filter output, *Cyan* = interference at isolation switch output.

The improvements for interference at other frequency offsets are tabulated in Table 1. The maximum improvement will be limited to either the filter rejection at the centre frequency of the interference or the isolation of the isolation switch, whichever is the least. Since several high isolation switches can be ganged in series, it is the filter rejection that sets the practical limit on interference rejection.

Frequency offset of Interference	Filter rejection wrt pass band [dB]	Improvement of in-band interference rejection [dB]
- 80MHz	102.9	44, 62 <sup>(1)</sup>
-60MHz	54.8	49, 53 <sup>(1)</sup>
-40MHz	26.6	24.8
-20MHz	7.2	7.0
+20MHz	5.4	5.0
+40MHz	15.3	14.0
+60MHz	24.4	21.2
+80MHz	32.6	27.0

+100MHz	40.0	29.7
+120MHz	46.6	31.0

Table 1: Improvement of in-band rejection of interference versus offset frequency.

<sup>(1)</sup> the greater degree of rejection of in-band interference results from extending the nesting to 50ns. Very high levels of interference rejection are achieved in these cases due to the high filter rejection close to zero Hertz.

These results are given for simple, unmodulated pulses. If intra-pulse modulations are used for the purposes of pulse compression, there will be additional spectral components within the IF pass band, however, these would also be rejected by the levels given in Table 1.

## 5 Conclusions

A full solution to the rejection of mutual interference entails spectral containment of the transmitted pulses through pulse shaping and rejection within the receiver. The use of two switches with a band pass filter between them as part of a typical superheterodyne receiver architecture can provide a high degree of rejection of neighbouring-channel interference. The rejection of interference is dependent on the non-dispersive nature of the circuitry between the two switches, the characteristics of the filter and the relative timings of the gating functions to the switches; the gating of the second switch being nested within the gating timings of the first. Rejection of in-band, co-channel, spectral components of mutual interference up to the level of the filter rejection at the centre frequency of the interference is possible. This offers considerable improvements over filtering on its own and would probably be beneficial in suppressing *all* forms of interference. A small increase in eclipsing losses is incurred due to the nesting margins between the two gating signals.

## Acknowledgements

I would like to acknowledge the invaluable contribution to this work of the late Chris Bourne, an ex-colleague and friend.

## References

- [1] D. Emery. "The Digital Synthesis of HF Surfacewave Radar Waveforms", *MSC thesis, Cranfield University, Shrivensham, UK*, (2004).
- [2] C. M. Alabaster. "Pulse Doppler Radar", *Scitech (now IET)*, (2012).
- [3] IEEE Std. 521-2002 "Standard Letter Designations for Radar-Frequency Bands". (1976, revised 1984, 2002).
- [4] James W. Nilsson, "Electric Circuits", 4<sup>th</sup> Ed., Addison-Wesley, ISBN 0-201-58179-5 (1993).
- [5] David Lynch, Jr and Carlo Kopp, "Multifunctional Radar Systems for Fighter Aircraft", chapter 5 in "Radar Handbook" 3<sup>rd</sup> Edition, Ed M. I. Skolnik, *McGraw-Hill*, ISBN 978-0-07-148547-0 (2008).